6348 *Macromolecules* **2009**, *42*, 6348–6360
DOI: 10.1021/ma901094s

Macromolecules
ARTICLE

Thermodynamic Components of the Atom Transfer Radical Polymerization Equilibrium: Quantifying Solvent Effects

Wade A. Braunecker,[†] Nicolay V. Tsarevsky,[†] Armando Gennaro,[‡] and Krzysztof Matyjaszewski*,[†]

[†]*Department of Chemistry, Carnegie Mellon University, 4400 Fifth Avenue, Pittsburgh, Pennsylvania 15213, and* [‡]*Dipartimento di Scienze Chimiche, Università di Padova, via Marzolo 1, 35131 Padova, Italy*

Received May 19, 2009

ABSTRACT: A thermodynamic scheme representing the atom transfer radical polymerization (ATRP) equilibrium as the formal sum of equilibria involving carbon−halogen bond homolysis and three additional distinct thermodynamic contributions related to the catalyst is rigorously evaluated. The reduction/oxidation of both the metal complex and the halogen atom, and the affinity of the higher oxidation state of the catalyst for halide anions (or "halidophilicity"), are measured. The validity and self-consistency of the model are verified by independently measuring, computing, or calculating the overall ATRP equilibrium constant and all four contributing equilibrium constants for one catalyst/alkyl halide combination in acetonitrile. As a thorough demonstration of the value and effectiveness of the scheme, the different equilibrium constants were measured or calculated in 11 different organic solvents, and a comparison of their values was used to both understand and predict catalyst activity in ATRP with high accuracy. The scheme explains quite well, for example, why the ATRP equilibrium constant is greater in dimethyl sulfoxide than in acetone by a factor of about 80 and why in acetonitrile and three different alcohols it is nearly identical. The solvent effects are also quantitatively analyzed in terms of Kamlet−Taft parameters, and linear solvation energy relationships are employed to extrapolate catalyst activity over 7 orders of magnitude in 17 more organic solvents and water.

Introduction

Control over polymer molecular weights and molecular weight distributions in all controlled radical polymerization (CRP) techniques is established through a dynamic equilibrium between dormant species and propagating radicals.[1] One advantage of atom transfer radical polymerization (ATRP)[2] over other CRP processes is that the ATRP equilibrium (Scheme 1), which governs the rate of polymerization, can be appropriately adjusted for a given reaction system by rationally modifying the structure of the transition metal-based catalyst to affect its activity.[3,4] In this way, control has been established over the polymerization of a wide variety of monomers with very different reactivities.[5,6]

While solvent effects on radical reactions are generally quite small, it has been observed that ATRP is subject to a significant acceleration in rate in the presence of water[7] and in some organic solvents like DMSO,[8] as compared to a solvent such as acetonitrile.[8] The primary aim of this work is to verify whether solvent effects on the rate of polymerization in ATRP can be explained and predicted with a thermodynamic scheme representing the ATRP equilibrium as the formal sum of an equilibrium involving carbon−halogen homolysis and three additional distinct thermodynamic contributions related to the catalyst: the reduction/oxidation of (i) the metal complex and (ii) the halogen atom and (iii) the affinity of the higher oxidation state of the catalyst for halide anions (or "halidophilicity").

The paper is divided into five major sections with distinct objectives. The first section investigates and quantifies accurately the solvent dependence of the ATRP equilibrium constant in 11 different organic solvents. In the second section, the thermodynamic scheme that will be used to ultimately explain and predict the solvent effects, a model which has previously been proposed in the literature,[9] is rigorously evaluated for the first time with one catalyst/alkyl halide combination in one solvent (acetonitrile). In the third section, the solvent-dependent equilibrium constants involving electron transfer, namely the reduction/oxidation of both the metal complex and the halogen atom, are quantified with knowledge of relative solvation energies available in the literature. The solvent dependence of the association equilibrium constant known as halidophilicity is quantified in the fourth section. Finally, all the thermodynamic components of the model measured in the preceding sections are collectively employed to explain the observed solvent effects in ATRP. The effects are also quantitatively analyzed in terms of Kamlet−Taft parameters, and linear solvation energy relationships are employed to extrapolate catalyst activity over 7 orders of magnitude in 17 more organic solvents and water. This work is an extension of preliminary results reported by us recently.[10]

Background

The ATRP equilibrium (characterized by the equilibrium constant K_{ATRP}) is established through homolytic cleavage of a C−X bond in an alkyl halide R−X by a transition metal complex activator Mt^zL_n (with a rate constant k_{act}) that generates the corresponding higher oxidation state metal halide complex deactivator $XMt^{z+1}L_n$ and an organic radical $R^\bullet$ (Scheme 1).[5,6] $R^\bullet$ can then propagate in the presence of a vinyl monomer M (k_p), terminate as in conventional free radical polymerization by coupling or disproportionation (k_t), or be reversibly deactivated by $XMt^{z+1}L_n$ to form a halide-capped dormant polymer chain (k_{deact}). The ligand L dramatically affects the values of both rate constants k_{act}[11] and k_{deact}[12] and therefore their ratio, K_{ATRP}. While it is easier to rationalize the effect of the ligand structure on thermodynamic rather than kinetic parameters,[3,4] the former being the focus of this paper, it is worth noting that "control"

*Corresponding author. E-mail: km3b@andrew.cmu.edu.

 Published on Web 07/02/2009

Scheme 1. ATRP Mechanism

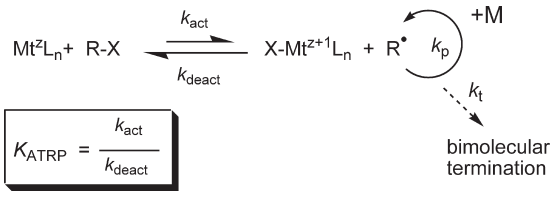

over polydispersity and molecular weights of polymers produced in ATRP is dramatically affected by the absolute values of k_{act} and k_{deact} of a given catalyst.[12] However, the rate of polymerization is governed by the position of the ATRP equilibrium, as illustrated in eq 1 for a particular monomer, M. Quantifying K_{ATRP} for a given catalyst therefore provides an excellent measure of the catalyst's true activity in polymerization.[13]

$$R_p = k_p[M][R^\bullet] = k_p[M]K_{ATRP}\frac{[RX][Mt^zL_n]}{[XMt^{z+1}L_n]} \quad (1)$$

The overall K_{ATRP} (Scheme 2a) is defined by the relative bond strengths toward homolysis of the alkyl halide (R−X) and the Mt^{z+1}−X bond of the ATRP deactivator (Scheme 2b) and formally can be expressed as the product of these two equilibria according to eq 2

$$K_{ATRP} = K_{BH}K_{Halo} \quad (2)$$

where K_{BH} characterizes the C−X bond homolysis in R−X and K_{Halo} characterizes the formation of the Mt^{z+1}−X bond or "halogenophilicity" of the catalyst (which is inverse of the equilibrium constant of Mt^{z+1}−X bond homolysis). Note that the term "halogenophilicity" refers to formation of a Cu^{II}−X bond from Cu^I and a halogen atom $X^\bullet$, whereas "halidophilicity" discussed later refers to donor−acceptor formation of Cu^{II}−X bond from Cu^{II} and a halide anion X^-. This treatment of K_{ATRP} has been experimentally verified in the literature, where a linear correlation was first observed[14] between values of K_{ATRP} measured with one Cu catalyst[13] (constant K_{Halo}) and six alkyl bromides, whose values of K_{BH} were calculated using DFT.[15] The correlation in eq 2 was later more extensively verified for 30 catalyst/alkyl halide combinations where values of K_{BH} were attained with high-level *ab initio* calculations.[12,16]

The halogenophilicity of a metal catalyst can in turn be represented as the product of three additional equilibria[9] (Scheme 2c and eq 3): (i) oxidation of the metal complex (or equilibrium of electron transfer, $1/K_{ET}$); (ii) reduction of a halogen atom to a halide ion (or electron affinity, K_{EA}); and (iii) association of the halide ion to the higher oxidation state metal complex $Mt^{z+1}L_n$ (or "halidophilicity", K_{Halido}). The ATRP process involves concerted inner-sphere electron transfer.[16] Thus, Scheme 2 provides only a formal representation of the thermodynamic components of the ATRP equilibrium, and the reactions represented do not necessarily take place as such.

$$K_{ATRP} = \frac{K_{BH}K_{EA}K_{Halido}}{K_{ET}} \quad (3)$$

This treatment of the ATRP equilibrium suggests that for a given alkyl halide (where K_{BH} and K_{EA} are constant) a linear correlation will exist between K_{ATRP} and the redox potential of a series of catalysts when their affinities for halide anions are similar. Indeed, among structurally related complexes of the same metal, a good correlation has been observed between the reducing power of a catalyst and the rate at which it catalyzes ATRP for a series of Cu-,[17−21] Fe-,[22,23] and Ru-based catalysts.[24]

Scheme 2. Representation of ATRP Equilibrium as a Thermochemical Cycle

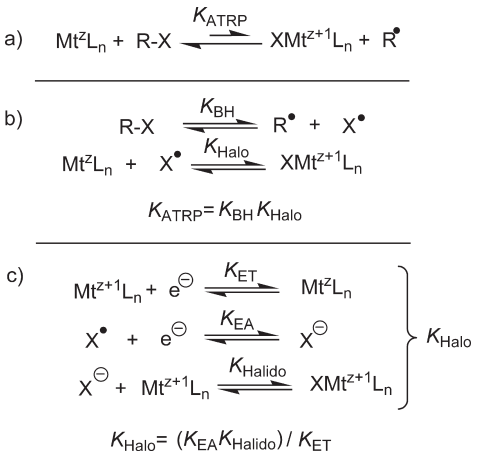

The redox potentials of Ru compounds have also been correlated with their catalytic activity in the related process atom transfer radical addition (ATRA).[25] A near perfect linear correlation was observed between logarithmic values of K_{ATRP} measured for 12 Cu^IBr-based catalysts with nitrogen-based ligands and their values of $E_{1/2}$ (directly related to K_{ET} by the Nernst equation) measured by cyclic voltammetry.[12] Most recently, apparent rate constants of ATRP for a methacrylate-based monomer were well correlated with the redox properties of several Cu-based catalysts in several solvent systems.[26] All of these results lend very credible support to the legitimacy of eq 3. However, the true validity of the equation has never been fully verified by independently measuring all five equilibrium constants and/or determining their values in different solvents.

Experimental Section

Materials. All reagents employed in this study were obtained from commercial sources at the highest available purity and used without further purification. All solvents were dried over sodium sulfate prior to use. Tris(2-pyridylmethyl)amine (TPMA) was synthesized according to a literature procedure.[27] All liquid reagents (HMTETA, the initiator MBriB, and the solvents) were deoxygenated by purging with nitrogen for 3 h prior to use.

Cyclic Voltammetry. All voltammograms were recorded at 25 °C with a Gamry Reference 600 potentiostat. Solutions of $Cu^{II}Br_2$/HMTETA (1.0 mM) were prepared in dry solvent containing 0.1 M Bu_4NClO_4 as the supporting electrolyte. Measurements were carried out under nitrogen at a scanning rate of 0.1 V s^{-1} using a glassy carbon disk as the working electrode and a platinum wire as the counter electrode. Potentials were measured vs Ag^+/Ag using 0.01 M $AgClO_4$ and a 0.1 M Bu_4NClO_4 salt bridge to minimize contamination of the analyte with Ag^+ ions.

Diffusion-Ordered NMR Spectroscopy (DOSY-NMR). Solutions of methyl isobutyrate were prepared in five deuterated solvents (acetone-d_6, DMSO-d_6, CD_3OD, DMF-d_7, and CD_3CN) in NMR tubes. The solutions were inserted in a Bruker NMR spectrometer operating at 500 MHz, and the temperature inside the spectrometer was kept at 22 ± 1 °C. The diffusion time Δ in the experiments was 70 ms for all solvents except DMSO, for which Δ = 100 and 120 ms was used, and the duration of the sinusoidal gradient pulses was δ = 1 ms, with a delay for gradient recovery time of 20 μs. For processing, the XWINNMR 3.5 NMR package with T1/T2 relaxation routine was used, and an exponential curve for the NMR signal intensity as a function of the gradient magnitude was used to fit the data and determine the diffusion coefficient.

General Procedure for the Determination of ATRP Equilibrium Constants (K_{ATRP}). $Cu^{I}Br$ (0.0072 g, 0.05 mmol) was added to a Schlenk flask joined with a quartz UV cuvette. After the flask was evacuated and backfilled with nitrogen five times, deoxygenated solvent (10 mL) was added through the side arm of the flask via a nitrogen-purged syringe. One equivalent of the ligand, e.g., HMTETA (13.6 μL, 0.05 mmol), was then added using a nitrogen-purged microsyringe. The contents were stirred for several hours (or overnight in the case of propylene carbonate and 1-PrOH) to ensure complete dissolution of $Cu^{I}Br$ and formation of the complex. The flask was then transferred to a UV/vis spectrometer, and the absorbance of the solution at λ_{max} of $Cu^{II}Br_2$/HMTETA was set to zero. Methyl 2-bromoisobutyrate (MBriB) (129 μL, 1.0 mmol) was injected into the Schlenk flask, and the absorbance corresponding to $Cu^{II}Br_2$/HMTETA generated due to the persistent radical effect was monitored with time. The concentration of the deactivator was calculated using values of the extinction coefficients for the $Cu^{II}Br_2$/HMTETA complexes determined separately (ε_{733} in PC = 269 M^{-1} cm^{-1}; ε_{765} in acetone = 223 M^{-1} cm^{-1}; ε_{715} in MeOH = 253 M^{-1} cm^{-1}; ε_{725} in EtOH = 268 M^{-1} cm^{-1}; ε_{725} in 1-PrOH = 271 M^{-1} cm^{-1}; ε_{730} in 2-PrOH = 274 M^{-1} cm^{-1}; ε_{730} in DMF = 239 M^{-1} cm^{-1}; ε_{730} in MeCN = 259 M^{-1} cm^{-1}; ε_{727} in NMP = 125 M^{-1} cm^{-1}; ε_{715} in DMSO = 275 M^{-1} cm^{-1}; ε_{745} in DMA = 264 M^{-1} cm^{-1}). Two measurements were performed with each complex, and the average value of K_{ATRP} is reported. The solvent dependence of the rate constant of termination k_t for small molecules used in the determination of K_{ATRP} is considered in these calculations and discussed in detail in the main text. The values of k_t for the methyl ester of the 2-isobutyryl radical $Me_2C^{\bullet}CO_2Me$ ($MiB^{\bullet}$) were calculated using the values of the diffusion coefficient of the stable structural analogue, methyl isobutyrate, as described in the following section and in more detail in the Supporting Information.

Results and Discussion

A. Solvent-Dependent Values of K_{ATRP}. Knowing the rate constant of termination for small molecules in a given solvent, K_{ATRP} in Schemes 1 and 2a can be accurately calculated by mixing Cu^{I} activator with R−X initiator and then monitoring $XCu^{II}L_n$ deactivator concentration as it accumulates with time. The $XCu^{II}L_n$ concentration can be easily determined from electronic spectroscopy, for example, by monitoring its absorbance at a wavelength for which the extinction coefficient was determined independently. Precise equations were recently derived based on the persistent radical effect to measure K_{ATRP} in this fashion, and the wide applicability of the approach was demonstrated.[13]

These equations are discussed in detail in the Supporting Information (eqs S1 and S2). Additionally, a value of k_t for small radicals must be known to use these equations. Originally, a constant value of k_t (2.5×10^9 M^{-1} s^{-1}) had been assumed for small radicals in the determination of K_{ATRP};[13] however, it is desirable to use more accurate solvent-dependent values. The determination of k_t from diffusion-ordered NMR spectroscopy is discussed in the Supporting Information, and a summary of the results is provided in Table 1 together with values of K_{ATRP}.

The equilibrium constants K_{ATRP} for the reactions of MBriB with $Cu^{I}Br$/HMTETA in these solvents were measured and calculated by means of the linear dependence in eq S2 (e.g., see Figure 1) and are presented in Table 1. All data used in the determination of K_{ATRP} can be found in the Supporting Information, including DOSY NMR curves and electronic absorption spectra of the deactivator.

The $Cu^{I}Br$/HMTETA and $Cu^{I}Br$/TPMA complexes used throughout this article were chosen specifically because the Cu^{I} species do not significantly disproportionate in any of the solvents employed, not even in pure water[30] (in contrast to many of the complexes employed in ATRP, e.g., complexes with *N,N,N′,N″,N″*-pentamethyldiethylenetriamine (PMDETA) or tris[2-(dimethylamino)ethyl]amine (Me_6TREN)). Significant disproportionation would ultimately complicate any measurements of K_{ATRP}, as Cu^{II} would accumulate via competing mechanisms. In addition, the precipitated Cu^0 would scatter light, leading to erroneous absorbance values which are ultimately used to determine the Cu^{II} concentration and K_{ATRP}.[8,31] The HMTETA and TPMA ligands, which form stable Cu complexes, have proven particularly useful in the ATRP of coordinating monomers such as 4-vinylpyridine.[32] Additionally, because of the high stability of the Cu^{I} and Cu^{II} TPMA complexes, this ligand is particularly useful for carrying out ATRP reactions at very low catalyst concentration.[33,34]

Values of K_{ATRP} for the HMTETA complex of $Cu^{I}Br$ in the different solvents vary by more than a factor of 80, with the lowest measured in acetone and the highest in DMSO. Values in MeCN and the three alcohols are nearly identical.

It should be noted that in solvents where halidophilicity is rather low (i.e., in MeOH, DMF, and DMSO; vide infra), some $[Cu^{II}Br/HMTETA]^+$ generated during the K_{ATRP} measurement experiment may dissociate to form

Table 1. Estimated Termination Rate Constants of $MiB^{\bullet}$ and Values of K_{ATRP} for the Reaction of MBriB with $Cu^{I}Br$/HMTETA in Various Solvents

solvent	viscosity [cP][a]	$D \times 10^5$ [cm^2 s^{-1}][b]	$2k_t \times 10^{-9}$ [M^{-1} s^{-1}][c]	K_{ATRP}	$K_{ATRP,rel}$
$(CD_3)_2CO$	0.326	3.4	7.40		
Me_2CO	0.303	*3.67*	7.98	3.14×10^{-9}	1.0
2-PrOH	2.044	*0.75*	1.63	6.89×10^{-9}	2.2
EtOH	1.083	*1.20*	2.61	7.46×10^{-9}	2.4
CD_3CN	0.357	3.1	6.74		
MeCN	0.339	*3.30*	7.16	7.49×10^{-9}	2.4
1-PrOH	1.943	*0.78*	1.70	8.52×10^{-9}	2.7
CD_3OD	0.602	2.12	4.61		
MeOH	0.551	*2.13*	4.63	9.27×10^{-9}	3.0
DMA	0.927	*1.36*	2.96	1.91×10^{-8}	6.1
PC	2.53	*0.65*	1.41	3.45×10^{-8}	11
DMF-d_7	0.885	1.42	3.09		
DMF	0.802	1.54	3.35	4.60×10^{-8}	15
NMP	1.67	*0.87*	1.89	1.39×10^{-7}	44
DMSO-d_6	2.180	0.64	1.39		
DMSO	1.99	*0.77*	1.68	2.61×10^{-7}	83

[a] At 25 °C. The values for deuterated solvents and protonated acetonitrile are taken from ref 28 and those for the other solvents from ref 29. [b] Diffusion coefficients of MiB. The values given in italics are calculated from the linear dependence of D (as determined by diffusion-ordered NMR spectroscopy) on viscosity of five deuterated solvents at 22 ± 1 °C. [c] Calculated from eq S5.

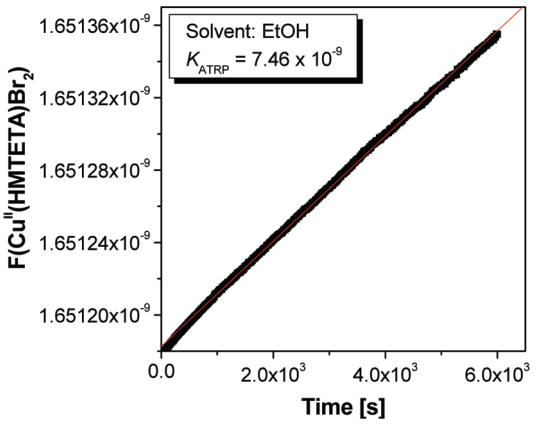

Figure 1. Plot of F[$Cu^{II}Br_2$/HMTETA] against time from eq S2 used in the determination of K_{ATRP} for the reaction of $Cu^{I}Br$/HMTETA with MBriB in ethanol.

$[Cu^{II}/HMTETA]^{2+}$. The latter complex is incapable of participating in the ATRP equilibrium, yet it has a similar extinction coefficient as the former. The concentration of $[Cu^{II}Br/HMTETA]^{+}$ monitored with time used to determine K_{ATRP} may therefore be slightly overestimated in these solvents. In practice, determination of K_{ATRP} was achieved by reacting ligated $Cu^{I}Br$ (5 mM) with MBriB (5−100 mM), as described in the Experimental Section. For solvents where the halidophilicity of $Cu^{II}L_n$ exceeds 10^4 M^{-1}, already at total concentration of Cu^{II} species ($[Cu^{II}L_n]_{tot} = [Cu^{II}L_n] + [BrCu^{II}L_n]$) equal to 0.5 mM, corresponding to 10% conversion of the starting Cu^{I} complex, more than 64% of the Cu^{II} species are bound to a halide ligand, and the error in the experimental K_{ATRP} values obtained by using the extinction coefficient of the Cu^{II} halide complex will be small. If deviation from linearity is observed in the plots of $F([XCu^{II}L_n])$ from eq S1 or S2 against time, the portion of the function corresponding to conversions of Cu^{I} to Cu^{II} exceeding 10−20% should only be analyzed.

A thermodynamic model representing the ATRP equilibrium constant as the formal product of equilibrium constants involving C−X bond homolysis and three additional thermodynamic contributions related to the catalyst is now explored in detail to rationalize these solvent effects on K_{ATRP} recorded in Table 1.

B. Quantifying Formally Contributing Equilibria. This section aims to verify the validity of eqs 2 and 3 as well as the entire model illustrated in Scheme 2 for a single catalyst/alkyl halide combination. For this purpose we chose $Cu^{I}Br$ with the 2,2′-bipyridine (bpy) ligand and methyl 2-bromoisobutyrate (MBriB) as the alkyl halide initiator, since several of the necessary data are already available in the literature. The section also serves to demonstrate the techniques that are used throughout this work to measure the solvent dependence of the different thermodynamic contributions to K_{ATRP}. The five equilibrium constants in eq 3 are all measured, computed, or calculated below under the same conditions (i.e., 22 ± 2 °C in MeCN) using $Cu^{I}Br$ with the 2,2′-bipyridine (bpy) ligand and methyl 2-bromoisobutyrate (MBriB) as the alkyl halide initiator. Once all five of these constants are obtained, there are a number of ways in which the self-consistency of the model can be verified; e.g., the measured value of K_{ATRP} can be compared with that predicted from the product of $(K_{BH}K_{EA}K_{Halido})/K_{ET}$ in eq 3.

Additionally, the value of a sixth equilibrium constant, that for halogenophilicity of the catalyst (K_{Halo}), can be calculated with two independent equations (K_{Halo} = K_{ATRP}/K_{BH}, and $K_{Halo} = (K_{EA}K_{Halido})/K_{ET}$, discussed in the Introduction), and their values compared to verify the self-consistency of Scheme 2. K_{Halo} is a true measure of the thermodynamic catalyst activity in ATRP but is difficult to measure experimentally, and computation is complicated since it involves reorganization of the transition metal complex, including an expansion of its coordination sphere, change in the oxidation state, and any specific solvation. Thus, having multiple routes to calculate K_{Halo} is of fundamental importance to ATRP catalyst development.

B.1. ATRP Equilibrium Constant (K_{ATRP}). As discussed in the first results section, K_{ATRP} can be accurately calculated by mixing Cu^{I} activator with R−X initiator and then monitoring $XCu^{II}L_n$ deactivator concentration as it accumulates with time, provided the rate constant of termination for small molecules is known for the given solvent. Using 1:1 stoichiometry ($[Mt^{z}L_n]_0 = [RX]_0$), values of the function $F([XMt^{z+1}L_n])$ defined in eq S1 were plotted against time, and K_{ATRP} was obtained from the slope of the linear dependence. In this way, K_{ATRP} was measured at room temperature (22 ± 2 °C) in MeCN for $Cu^{I}Br(bpy)_2$ with ethyl 2-bromoisobutyrate (EBriB)[13] as $3.9 \times 10^{-9} = 10^{-8.4}$, which is expected to have similar thermodynamic value (K_{BH}) as MBriB used elsewhere in this work. Values of K_{ATRP} must be this low ($\sim 10^{-9}-10^{-4}$) to keep radical concentrations low and minimize termination reactions.

B.2. Alkyl Halide Bond Homolysis (K_{BH}). The C−X bond dissociation or homolysis free energy (ΔG_{BH}) for the alkyl halide in the process characterized by K_{BH} can be accessed computationally not only in vacuum but also in a solvent. For MBriB, ΔG_{BH} was computed at 25 °C in MeCN as 215.9 kJ mol^{-1}, with the corresponding value of $K_{BH} = 10^{-37.8}$ M. This value was obtained from high-level *ab initio* calculations described in a recent study.[16] In that work, the free energies were calculated at the G3(MP2)-RAD level of theory, and solvation effects were incorporated via the CPCM continuum model.

B.3. Electron Affinity of Halogen Atom (K_{EA}). The Gibbs energy of transfer (also known as the solvent medium effect) can be defined as the change in total solvation energy (or chemical potential) of a solute when it is transferred from one solvent to another. The magnitude of this effect defines the relative stability of the solute in the two solvents and thus determines the consequences of changing the solvent on the redox characteristics of the solute.[35] Knowing the value of the redox potential $E^{\circ}_{Br^{\bullet}/Br^{-}}$ in water (2.00 V vs SHE) (see the Supporting Information), it is possible to calculate K_{EA} for bromine in any solvent with knowledge of the Gibbs energy of transfer ($\Delta_{tr}G^{\circ}_{(Br^{-},W\rightarrow S)}$) of Br^{-} from water to that solvent using the equations

$$\Delta G^{\circ}_{(EA,S)} = \Delta G^{\circ}_{(EA,W)} + \Delta_{tr}G^{\circ}_{(X^{-},W\rightarrow S)} = -FE^{\circ}_{X^{\bullet}/X^{-}} + \Delta_{tr}G^{\circ}_{(X^{-},W\rightarrow S)} \quad (4)$$

$$RT \ln K_{EA} = -\Delta G^{\circ}_{(EA,S)} \quad (5)$$

Fortunately, ($\Delta_{tr}G^{\circ}_{(Br^{-},W\rightarrow S)}$) values are widely available for different solvents.[36] The assumption is made in these calculations that $\Delta_{tr}G^{\circ}_{(Br^{\bullet},W\rightarrow S)}$ of the neutral bromine atom is practically null and can therefore be neglected, since the solvation energy will not vary much among the different polar solvents. Indeed, a series of studies by Svaan and Parker have shown that both the entropy and enthalpy contribution to the redox potential of a particular species closely follows the charge localization.[37,38] Coullerez et al.

have commented that this indicates the relatively weak solvation of neutral molecules and radicals can be regarded as solvent independent and that the main contribution to the solvent effect on the redox potential of these species will originate from differences in ion solvation.[39]

For the half-reaction in these calculations ($Br^{\bullet} + e^- = Br^-$), $\Delta G^\circ_{(EA,S)}$ and K_{EA} are reported vs SHE convention (i.e., taking $\Delta G^\circ = 0$ for the process $H^+_{(W)} + e^- = {}^1/_2H_{2(g)}$). Using eqs 4 and 5, along with $E^\circ_{Br^{\bullet}/Br^-} = 2.00$ V vs SHE in water and $\Delta_{tr}G^\circ_{(Br^-,W\rightarrow MeCN)} = 31.3$ kJ mol^{-1},[36] $\Delta G^\circ_{(EA,MeCN)}$ for bromine in MeCN can be calculated as -161.67 kJ mol^{-1} (relative to SHE convention). This gives a value $K_{EA} = 10^{28.3}$ M^{-1} in MeCN.

B.4. Reduction/Oxidation of Metal Catalyst (K_{ET}). In similar fashion to the way that K_{EA} was calculated in MeCN vs SHE convention, K_{ET} for the Cu catalyst can be calculated by measuring its redox potential ($E_{1/2}$) vs a reference electrode (0.01 M Ag^+/Ag) in MeCN and calibrating this value vs SHE, knowing the free energy of transfer of Ag^+ from water to MeCN ($\Delta_{tr}G^\circ_{(Ag^+,W\rightarrow MeCN)} = -24.1$ kJ mol^{-1}).[36]

$$\Delta G^\circ_{(ET,S)} = -FE_{1/2} + \Delta G_{(Ref,W)} - \Delta_{tr}G^\circ_{(Ag^+,W\rightarrow S)} \quad (6)$$

Knowing $E^\circ_{Ag^+/Ag} = 0.799$ V vs SHE in water,[40] and neglecting the activity coefficient for Ag^+, the potential of the 0.01 M Ag^+/Ag reference electrode in water can be calculated as 0.681 V vs SHE ($\Delta G_{(Ref,W)} = -65.67$ kJ mol^{-1}). Having measured the $E_{1/2}$ of $[Cu^{II}(bpy)_2]^{2+}$ in MeCN at 25 °C in the absence of any halide anions as -0.159 V vs 0.01 M Ag^+/Ag, eq 6 can be used to calculate $\Delta G^\circ_{(ET,MeCN)}$ of $[Cu^{II}(bpy)_2]^{2+}$ as -26.23 kJ mol^{-1}. This gives a value $K_{ET} = 10^{4.60}$ M^{-1} in MeCN. Both K_{EA} and K_{ET} are referred to SHE convention. However, their ratio $K_{EA}/K_{ET}=10^{23.7}$ employed in eq 3 annuls the arbitrary reference value.

B.5. Halidophilicity of Cu^{II} (K_{Halido}). Typical values of K_{Halido} in aprotic solvents and solvents that do not coordinate strongly with Cu^{II} (hydrocarbons, ethers, ketones, DMF, etc.) are on the order of 10^4-10^5 M^{-1},[41] whereas in protic solvents and mixed aqueous solutions, these values are significantly lower ($10-10^3$ M^{-1}).[42] The equilibrium constant of halide anion coordination can be measured by spectroscopic means,[43] as described in the literature for bpy-based ATRP deactivators in several protic solvents.[42] The halidophilicity of $[Cu^{II}(bpy)_2]^{2+}$ toward both Br^- and Cl^- was studied in various water-containing mixed solvents, and it was shown that in all cases the values of K_{Halido} decreased significantly as the amount of water in the mixtures increased.[44] From this spectroscopic data, one can approximate, by means of extrapolation, the value of bromidophilicity of $[Cu^{II}(bpy)_2]^{2+}$ as $K_{Bromido} \approx 10^5$ M^{-1} in pure MeCN.

B.6. Calculating Halogenophilicity of the Cu-Based ATRP Catalyst. The relation among the five equilibrium constants discussed above (K_{ATRP}, K_{BH}, K_{EA}, K_{ET}, and K_{Halido}) measured for the $Cu^IBr(bpy)_2$ + MBriB system in MeCN at room temperature are illustrated in Figure 2. Halogenophilicity can be calculated from $K_{Halo} = K_{ATRP}/K_{BH}$ as $10^{29.4}$ M^{-1}. This value is in good agreement with that calculated from the other three equilibrium constants ($K_{Halo} = (K_{EA}K_{Halido})/K_{ET}$) as $10^{28.7}$ M^{-1}. Another way to compare the self-consistency of the data is to calculate alkyl halide bond dissociation energy for MBriB. Rearranging eq 3 to $K_{BH} = (K_{ATRP}K_{ET})/(K_{Halido}K_{EA})$, the C–Br BDE for MBriB can be calculated as $\Delta G_{BH} = 211.8$ kJ mol^{-1}, which corresponds to $K_{BH}=10^{-37.1}$ M. The value is in good agreement with that of 215.9 kJ mol^{-1} ($K_{BH}=10^{-37.8}$ M) calculated using high-level

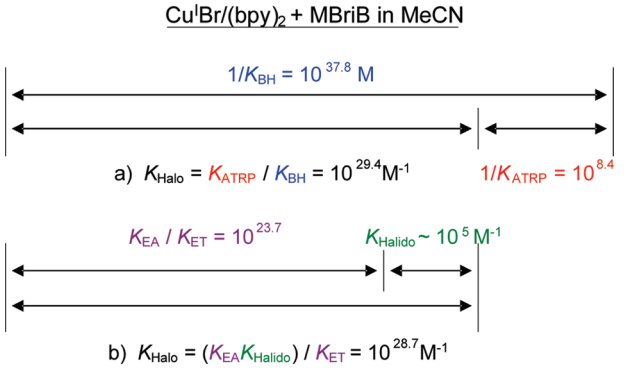

Figure 2. (a) K_{ATRP} measured for $Cu^IBr/(bpy)_2$ with EBriB in MeCN at rt as 3.9×10^{-9} (or $10^{-8.4}$);[13] alkyl halide bond dissociation energy of MBriB computed in MeCN as 215.9 kJ mol^{-1}, or $K_{BH}=10^{-37.8}$ M^{-1},[16] halogenophilicity calculated from $K_{Halo} = K_{ATRP}/K_{BH}$ as $10^{29.4}$ M^{-1}. (b) Bromidophilicity of $[Cu^{II}Br/(bpy)_2]^+$ estimated in MeCN as $\sim10^5$ M^{-1};[44] ratio of K_{EA} for Br^- and K_{ET} for $[Cu^{II}(bpy)_2]^{2+}$ in MeCN calculated as $10^{23.7}$; halogenophilicity calculated from $K_{Halo} = (K_{EA}K_{Halido})/K_{ET}$ as $10^{28.7}$ M^{-1}.

ab initio molecular orbital calculations that took MeCN solvent effects into account.[16] These results lend credible support to the validity of eqs 2 and 3 and the model in Scheme 2 for the $Cu^IBr(bpy)_2$ + MBriB system under these conditions in MeCN.

C. Solvent Effects on Electron Transfer Equilibria. The objective of the following section is to illustrate for a given catalyst how electron transfer equilibria are affected by solvent. Electrochemistry and knowledge of relative solvation energies are used to calculate K_{EA} for Br^- and $1/K_{ET}$ for the Cu complexes with HMTETA and TPMA. Ten different organic solvents are investigated, in which the value of the aforementioned equilibrium constants vary by as much as 5–6 orders of magnitude.

C.1. Solvent Dependence of Electron Affinity of Halogen Atom. As discussed above, the magnitude of the Gibbs energy of transfer of a solute from one solvent to another dictates the redox potential of the solute in the different solvents.[35] Knowing $E^\circ_{X^{\bullet}/X^-}$ in water (see the Supporting Information), it is possible to calculate K_{EA} from the Gibbs energies of transfer ($\Delta_{tr}G^\circ_{(X^-,W\rightarrow S)}$) of X^- from water to a given organic solvent[36] using eqs 4 and 5. Again, as the main contribution to the solvent effect on the redox potential of these species will originate from differences in ion solvation, the assumption is made in these calculations (which was discussed earlier and can be justified in the literature)[39] that $\Delta_{tr}G^\circ_{(Br^{\bullet},W\rightarrow S)}$ of the neutral bromine atom will not be considered, since the solvation energy does not vary much among the different polar solvents and can therefore be neglected.

The solvents in this study were specifically chosen to represent a broad range of K_{EA} values. For the half-reactions in these calculations, $\Delta G^\circ_{(EA,S)}$ and K_{EA} are reported vs SHE convention (i.e., $H^+_{(W)} + e^- = {}^1/_2H_{2(g)}$, $\Delta G^\circ = 0$). As can be seen in Table 2, values of K_{EA} for the bromine span more than 7 orders of magnitude. The transfer energies used in the calculations, as well as values of $\Delta G^\circ_{(EA,S)}$ calculated using eq 4, are provided alongside the values of K_{EA} as a matter of convenience for anyone attempting to reproduce the calculations.

C.2. Solvent Dependence of Electron Transfer of Copper Complexes. As has been demonstrated in the literature, a linear correlation exists between K_{ATRP} and $E_{1/2}$ values for a series of $Cu^{II}Br_2$/L catalysts in MeCN.[12] The $E_{1/2}$ values of Cu complexes used as ATRP catalysts are quite solvent

dependent.[21,39] However, the redox potential of a single catalyst has not been compared with its catalytic activity (i.e., K_{ATRP}) in a series of different solvents. In this section, Cu^{I}/L complexes with two different ligands are investigated (L = *N*,*N*,*N*′,*N*″,*N*‴,*N*‴-hexamethyltriethylenetetramine, or HMTETA, and tris[(2-pyridyl)methyl]amine, or TPMA). As mentioned, these complexes were chosen specifically because the Cu^{I} species do not significantly disproportionate in any of the solvents employed, not even in pure water. Values of $1/K_{ET}$ were quantified using cyclic voltammetry to measure the redox potentials of the $Cu^{II}(CF_3SO_3)_2$/L complex against the Ag^+/Ag couple. With knowledge of $\Delta_{tr}G^\circ_{(Ag^+,W\rightarrow S)}$[36] and $E^\circ_{Ag^+/Ag}$[40] in water vs SHE, $\Delta G^\circ_{(ET,S)}$ and $1/K_{ET}$ for the ATRP catalyst could ultimately be calculated (vs SHE convention) from eq 6 and are provided in Table 3.

The voltammograms of the $Cu^{II}(CF_3SO_3)_2$/L complex with TPMA in the different solvents are generally more reversible than those with HMTETA, as judged by the smaller values of ΔE_p (on average 83 mV for TPMA compared to 132 mV for HMTETA). As values of $E_{1/2}$ are a good approximation of the standard potential E° when the voltammograms are fully reversible, our assumption that $E_{1/2} \approx E^\circ$ in the calculation of $1/K_{ET}$ is more reliable for the case of TPMA than it is for HMTETA. Also, the TPMA complex is always more reducing than that with HMTETA, typically by 200 mV. Among the five solvents MeOH, EtOH, 1-PrOH, MeCN, and Me_2CO, one can see in Table 3 that the value of $\log(1/K_{ET})$ for the TPMA complex varies only by ~0.2. In propylene carbonate (PC), the complex is an order of magnitude more reducing, and in DMSO, DMF, and DMA, it is 3−4 orders of magnitude more reducing than in the first five solvents discussed. The strong reducing power of the complex in DMSO, DMF, and DMA reflects the stronger preferential solvation of the Cu^{II} oxidation state (vs Cu^{I}) in these solvents. Similar results were obtained for the HMTETA complex.

Table 2. Relative Values of K_{EA} for Bromine Calculated in Various Solvents at 25 °C[a]

solvent	$\Delta_{tr}G^\circ_{(Br^-,W\rightarrow S)}$ [kJ mol^{-1}][b]	$\Delta G^\circ_{(EA,S)}$ [kJ mol^{-1}][c,d]	$\log(K_{EA})$[e]
Me_2CO	42	−150.97	26.5
DMA	44.0	−148.97	26.1
NMP	37	−155.97	27.3
DMF	36.2	−156.77	27.5
MeCN	31.3	−161.67	28.3
PC	30.0	−162.97	28.6
DMSO	27.4	−165.57	29.0
1-PrOH	22	−170.97	30.0
EtOH	18.2	−174.77	30.6
MeOH	11.1	−181.87	31.9
water		−192.97	33.8

[a] All thermodynamic values for this half-reaction reported vs SHE convention (i.e., $H^+_{(W)} + e^- = {}^1/_2H_{2(g)}$, $\Delta G^\circ = 0$). [b] All $\Delta_{tr}G^\circ_{(Br^-,W\rightarrow S)}$ values obtained from the literature.[36] [c] Values of $\Delta G^\circ_{(EA,S)}$ calculated from $\Delta G^\circ_{(EA,S)} = -FE^\circ_{Br^\bullet/Br^-} + \Delta_{tr}G^\circ_{(Br^-,W\rightarrow S)}$. [d] $E^\circ_{Br^\bullet/Br^-} = 2.00$ V vs SHE in water.[45] [e] Values of K_{EA} calculated from $RT \ln K_{EA} = -\Delta G^\circ_{(EA,S)}$.

C.3. Calculating Halidophilicity. With known values of K_{ATRP} (Table 1), K_{EA} (Table 2), and K_{ET} (Table 3) for all studied solvents, and using the value of K_{BH}(MBriB) = 1.49×10^{-38} M in MeCN,[16] the true halidophilicity (in this case, bromidophilicity) of Cu^{II}/HMTETA can be calculated in all solvents using eq 3. The values are presented in Table 5 alongside apparent values calculated in the next section. The values of $K_{Bromido}$ can be used as a guide to selecting (co)solvents for maximizing halidophilicity, e.g., additives in ATRP in protic media. The solvents in which the halidophilicity is greater will be more suitable additives, not only due to increased catalytic activity (higher K_{ATRP} for higher K_{Halido}; cf. eq 3) but also because of better deactivation efficiency due to the lower propensity of the $XCu^{II}L$ to dissociate and form the complex $Cu^{II}L$, which is unable to deactivate radicals.[42] The lowest halidophilicity is observed in DMSO and the highest in Me_2CO and DMA. The halidophilicities in protic solvents such as MeOH, EtOH, and 1-PrOH that solvate halide ions and DMF that solvates or coordinates to Cu^{II} species are relatively low.

D. Electrochemical Measurements of Halidophilicity. *D.1. Apparent Values of Halidophilicity for Various Cu^{II}/L Complexes in MeCN*. The redox potential of the catalyst is related to the relative stabilization of the Cu^{II} vs Cu^{I} state upon complexation with a ligand. For ligands forming 1:1 complexes with copper ions, the following relation holds and

Table 3. $E_{1/2}$ and $1/K_{ET}$ Measured for $Cu^{II}(CF_3SO_3)_2$/L in Various Solvents at 25 °C[a]

solvent	ΔE_p [mV]	$E_{1/2}$ [V vs 0.01 M Ag^+/Ag]	$\Delta_{tr}G^\circ_{(Ag^+,W\rightarrow S)}$ [kJ mol^{-1}]	$\Delta G^\circ_{(ET,S)}$ [kJ mol^{-1}]	$\log(1/K_{ET})$
			L = HMTETA		
MeOH	99	−0.446	8.5[35]	−31.1	−5.46
EtOH	116	−0.429	4.5[35]	−28.8	−5.04
1-PrOH	150	−0.455	1[36]	−22.8	−3.99
MeCN	245	−0.243	−24.1[35]	−18.1	−3.18
Me_2CO	104	−0.491	9[36]	−27.3	−4.78
PC	140	−0.688	18.8[36]	−18.1	−3.17
DMSO	110	−0.295	−32.0[35]	−5.21	−0.913
NMP	110	−0.325	−26[36]	−8.32	−1.46
DMF	117	−0.409	−20.8[36]	−5.41	−0.948
DMA	99	−0.306	−29.0[36]	−7.15	−1.25
			L = TPMA		
MeOH	75	−0.670	8.5[35]	−9.53	−1.67
EtOH	89	−0.615	4.5[35]	−10.8	−1.90
1-PrOH	112	−0.590	1[36]	−9.75	−1.71
MeCN	69	−0.321	−24.1[35]	−10.6	−1.86
Me_2CO	77	−0.665	9[36]	−10.5	−1.84
PC	88	−0.835	18.8[36]	−3.91	−0.685
DMSO	81	−0.450	−32.0[35]	9.75	1.71
NMP		[b]	−26[36]		
DMF	71	−0.612	−20.8[36]	14.2	2.48
DMA	70	−0.553	−29.0[36]	16.7	2.93

[a] 0.1 M NBu_4ClO_4, 1.0 mM $Cu^{II}(CF_3SO_3)_2$/L, scan rate 0.1 V s^{-1}; potentials reported vs 0.01 M $AgClO_4$/Ag; $\Delta G^\circ_{(ET,S)}$ and $1/K_{ET}$ reported vs SHE convention; $\Delta G^\circ_{(ET,S)} = -FE_{1/2} + \Delta G_{(Ref,W)} - \Delta_{tr}G^\circ_{(Ag^+,W\rightarrow S)}$; $\Delta G_{(Ref,W)} = -65.673$ kJ mol^{-1} ($E_{Ag^+/Ag} = 0.681$ V vs. SHE); the activity coefficient for Ag^+ has been neglected. [b] Not reversible.

can be further simplified for relatively stable complexes:[46]

$$E = E^0 + \frac{RT}{F}\left(\ln\frac{[Cu^{II}]_{tot}}{[Cu^{I}]_{tot}} - \ln\frac{1+\beta^{II}[L]}{1+\beta^{I}[L]}\right) \approx E^0 + \frac{RT}{F}\left(\ln\frac{[Cu^{II}]_{tot}}{[Cu^{I}]_{tot}} - \ln\frac{\beta^{II}}{\beta^{I}}\right) \quad (7)$$

where β^j is the stability constant of the Cu^jL complex ($j = I$, II). By measuring $E_{1/2}$ of the Cu complexes in the presence and absence of Br^- anions, a ratio of the binding constant of Br^- with Cu^{II}/L to the binding constant of Br^- with Cu^{I}/L is obtained (i.e., a ratio of Cu^{II} halidophilicity to Cu^{I} halidophilicity). If Br^- coordination to the coordinatively saturated Cu^{I}/L cation is negligible, a good estimate of Cu^{II}/L halidophilicity can be obtained. This apparent halidophilicity value determined by electrochemical measurements is herein designated K^{app}_{Halido} to distinguish it from the pure halidophilicity K_{Halido} of $Cu^{II}L_n$.

More precisely, the ratio obtained from CV measurements is $(1 + K_{Halido}(Cu^{II}L_n)[X^-])/(1 + K_{Halido}(Cu^{I}L_n)[X^-])$, which can be approximated with $K_{Halido}(Cu^{II}L_n)$ when $K_{Halido}(Cu^{I}L_n)$ is very low. $K_{Halido}(Cu^{I}L_n)$ is the equilibrium constant of the process

$$X^- + Cu^{I}L_n \overset{K_{Halido}(Cu^{I}L_n)}{\rightleftharpoons} [X\cdots Cu^{I}L_n] \quad (8)$$

where charges of the complexes are omitted for simplicity and the symbol "$\cdots$" represents either a coordination bond or a tight ion pair. The true halidophilicity of the $Cu^{II}L_n$ complex, without "interference" from the halidophilicity of the $Cu^{I}L_n$ complex, can be determined from eq 3, provided that the values of K_{ATRP}, K_{BH}, K_{EA}, and K_{ET} are known, as is done in Table 5. If the value obtained by this approach is close to the one determined electrochemically, interaction (coordination or tight ion-pair formation) between $Cu^{I}L_n$ and halide anions is negligible.

Table S1 in the Supporting Information summarizes the cyclic voltammetric data recorded for 14 Cu catalysts in MeCN with the noncoordinating counterion $CF_3SO_3^-$. The majority of the complexes investigated showed good quasi-reversibility under these conditions as judged by their relatively low ΔE_p values. K_{ATRP} values in the table were taken from the literature for $Cu^{I}Br$/L complexes in MeCN with EBriB.[12] For reversible and quasi-reversible voltammograms where $E_{1/2}$ is a good approximation of the standard potential, a correlation should be observed between logarithmic values of K_{ATRP} and recorded $E_{1/2}$ values. The correlation will be linear when K_{BH}, K_{EA}, and K_{Halido} are constant. In Figure 3, values of K_{ATRP} were measured with $Cu^{I}Br$/L complexes and EBriB (constant K_{BH} and K_{EA}).[12] The poor correlation between logarithmic values of K_{ATRP} (for the reaction of $Cu^{I}Br$/L complexes with RBr) and values of $E_{1/2}$ of $Cu^{II}(CF_3SO_3)_2$/L complexes in Figure 3 (R^2 value from least-squares analysis = 0.58) suggests K_{Halido} for all the complexes is quite different.

When apparent values of halidophilicity are taken into account by measuring $E_{1/2}$ in the presence of Br^- and not assumed to be constant among all the complexes,[12] an excellent correlation is observed in Figure 3 between catalyst activity and redox potentials (R^2 value from least-squares analysis = 0.96). The $Cu^{II}Br_2$/L complexes are always more reducing than their $Cu^{II}(CF_3SO_3)_2$/L analogues, and the difference in measured $E_{1/2}$ values allows the calculation of apparent halidophilicities of the complexes. For most complexes with tetradentate ligands, where Cu^{I} is coordinatively saturated and Br^- serves as the counterion (as opposed to ligand), the difference in $E_{1/2}$ values is typically 240 mV, corresponding to an apparent halidophilicity of $\sim 10^4$ M^{-1} in MeCN. This value is consistent with typical values measured in aprotic solvents (10^4–10^5 M^{-1}).[41]

Table 4. $E_{1/2}$ and K^{app}_{Halido}/K_{ET} Measured for $Cu^{II}Br_2$/L in Various Solvents at 25 °C[a]

solvent	ΔE_p [mV]	$E_{1/2}$ [V vs 0.01 M Ag^+/Ag]	$\Delta_{tr}G^\circ_{(Ag^+,W\rightarrow S)}$ [kJ mol^{-1}]	$\Delta G^\circ_{(ET+Br,S)}$ [kJ mol^{-1}]	log (K^{app}_{Halido}/K_{ET})
			L = HMTETA		
MeOH	143	−0.497	8.5[35]	−26.2	−4.60
EtOH	194	−0.512	4.5[35]	−20.8	−3.64
1-PrOH	218	−0.523	1[36]	−16.2	−2.84
MeCN	155	−0.354	−24.1[35]	−7.42	−1.30
Me_2CO	115	−0.710	9[36]	−6.17	−1.08
PC	208	−0.828	18.8[36]	−4.58	−0.803
DMSO	126	−0.321	−32.0[35]	−2.70	−0.473
NMP	143	−0.445	−26[36]	3.26	0.572
DMF	130	−0.499	−20.8[36]	3.27	0.573
DMA	159	−0.466	−29.0[36]	8.29	1.45
			L = TPMA		
MeOH	77	−0.791	8.5[35]	2.15	0.376
EtOH	97	−0.782	4.5[35]	5.28	0.925
1-PrOH	157	−0.805	1[36]	11.0	1.93
MeCN	70	−0.575	−24.1[35]	13.9	2.44
Me_2CO	79	−0.908	9[36]	12.9	2.27
PC	79	−1.072	18.8[36]	19.0	3.32
DMSO	83	−0.525	−32.0[35]	17.0	2.98
NMP	90	−0.613	−26[36]	19.5	3.41
DMF	80	−0.695	−20.8[36]	22.2	3.89
DMA	84	−0.633	−29.0[36]	24.4	4.27

[a] 0.1 M NBu_4ClO_4, 1.0 mM $Cu^{II}Br_2$/L, scan rate 0.1 V s^{-1}; potentials reported vs 0.01 M $AgClO_4$/Ag; $\Delta G^\circ_{(ET+Br,S)}$ and K^{app}_{Halido}/K_{ET} reported vs SHE convention; $\Delta G^\circ_{(ET+Br,S)} = -FE_{1/2} + \Delta G_{(Ref,W)} - \Delta_{tr}G^\circ_{(Ag^+,W\rightarrow S)}$; $\Delta G_{(Ref,W)} = -65.673$ kJ mol^{-1} ($E_{Ag^+/Ag} = 0.681$ V vs. SHE); the activity coefficient for Ag^+ has been neglected.

Table 5. Apparent and Calculated Bromidophilicity of Cu^{II}/HMTETA Complexes in Various Solvents at 25 °C

solvent	$\log(K^{app}_{Bromido}/K_{ET}) - \log(1/K_{ET})$	log $K_{Bromido}$[a]
Me_2CO	3.70	7.78
DMA	2.70	5.33
PC	2.37	5.11
NMP	2.03	5.2
MeCN	1.88	4.66
DMF	1.52	4.11
EtOH	1.40	4.21
1-PrOH	1.15	3.93
MeOH	0.86	3.52
DMSO	0.44	3.23

[a] Calculated from eq 3 using data for K_{ATRP} (Table 1), K_{EA} (Table 2), K_{ET} (Table 3), and K_{BH}(MBriB) = 1.49×10^{-38} M (ref 16).

D.2. Apparent Values of Halidophilicity in Various Solvents. The remarkable correlation observed in Figure 3 between log(K_{ATRP}) and the redox potentials of the $Cu^{II}Br_2$/L complexes in MeCN prompted us to measure the redox potentials of the $Cu^{II}Br_2$/L complexes with TPMA and HMTETA in 10 different solvents. A summary is provided in Table 4, together with values of $\Delta G^\circ_{(ET+Br,S)}$ and K^{app}_{Halido}/K_{ET}.

The voltammograms of the $Cu^{II}Br_2$/TPMA complex in the different solvents are generally more reversible than those of $Cu^{II}Br_2$/HMTETA (ΔE_p on average 90 mV for TPMA compared to 159 mV for HMTETA). The equilibrium constant of electron transfer for $Cu^{II}Br_2$/TPMA spans nearly 4 orders of magnitude in these solvents, with the Cu^{I}/TPMA complex being the least reducing in the alcohols and most reducing in NMP, DMF, and DMA.

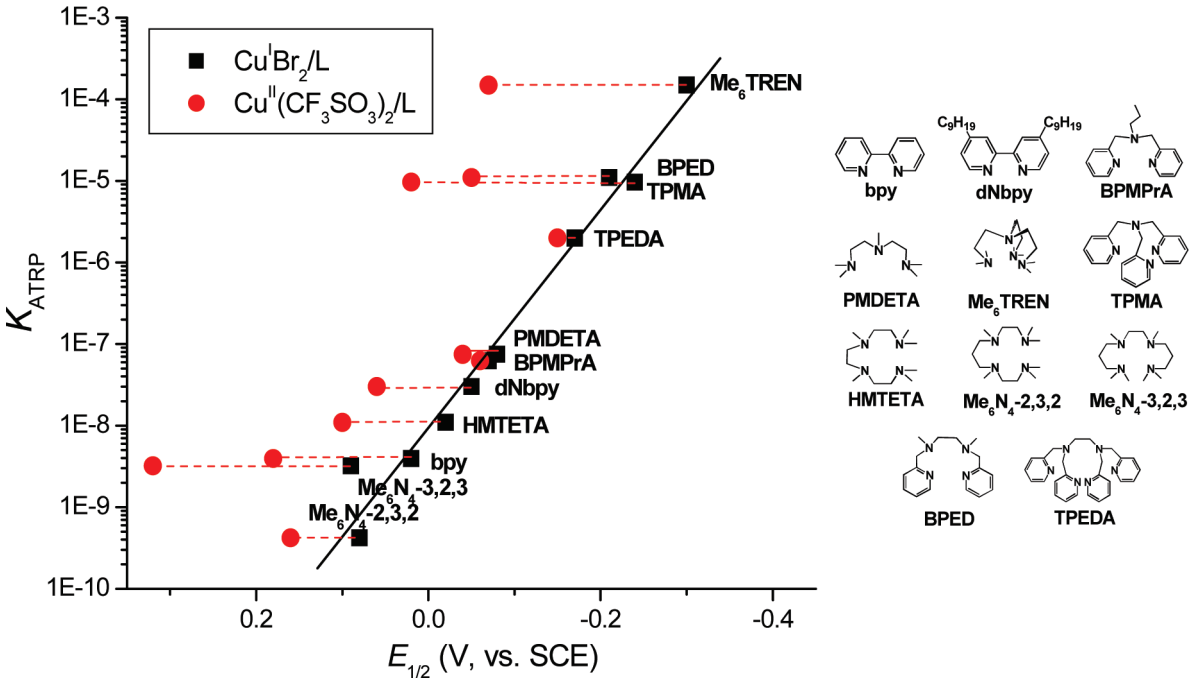

Figure 3. Comparison of $Cu^{II}(CF_3SO_3)_2$/L and $Cu^{II}Br_2$/L redox potentials correlated with values of K_{ATRP} (measured with EBriB) at rt in MeCN.

One can determine relative values of apparent halidophilicity in the different solvents by comparison of the data in Tables 3 ($1/K_{ET}$) and 4 (K^{app}_{Halido}/K_{ET}). A summary of apparent values of $K^{app}_{Bromido}$ is provided below in Table 5. Halidophilicity among the different solvents is a function of how well both the halide anion and the Cu^{II} species are solvated. For example, in the three alcohols, where the relative solvation of the Cu^{II} to Cu^{I} oxidation states were similar for the TPMA complex with a triflate counterion ($\log(1/K_{ET})$ varies by ~0.2), a systematic increase in reducing power can be seen for the bromide complex with TPMA on going from MeOH to EtOH to 1-PrOH that parallels the solvation strength of the halide anion by the alcohols.[36] In other words, as the bromide anion becomes more poorly solvated, it binds stronger to Cu^{II}, and the complex becomes more reducing. In the solvents DMSO and DMF, both the $Cu^{II}(CF_3SO_3)_2$/L and $Cu^{II}Br_2$/L complexes are very reducing. Despite the fact that the halide anion is more poorly solvated in these solvents than in alcohols, the Cu^{II} cation is apparently very well solvated, and halidophilicity remains low. The low apparent, electrochemically determined, values of K^{app}_{Halido} in most of the solvents may be a consequence of the fact that the halide anion coordinates/tightly associates to Cu^{I} as well (i.e., not only to Cu^{II}) in these solvents. The apparent halidophilicities in Table 5, calculated from $\log(K^{app}_{Bromido}/K_{ET}) - \log(1/K_{ET})$ and the data in Tables 3 and 4, are compared alongside the actual values of halidophilicity calculated in the previous section by rearranging eq 3 and knowing the values of the other four equilibrium constants ($K_{Bromido} = (K_{ATRP}K_{ET})/(K_{BH}K_{EA})$).

For eight of the organic solvents, the true halidophilicities are larger than the apparent ones by 2.6−2.8 orders of magnitude. For NMP and acetone, these values are higher (3.17 and 4.08, respectively), suggesting the affinity of the Cu^{I}(HMTETA) complex toward bromide anion is more significant in the latter two solvents. Recent EXAFS[47] and X-ray[48] studies indeed suggest that Cu^{I} complexes with tetradentate N-based ligands such as Me_6TREN or TPMA can coordinate to halide ions. It is noteworthy that although the true halidophilicities are larger than the apparent ones, the general trends in Table 5 are still seen. For instance, the lowest halidophilicity is observed in DMSO and the highest in Me_2CO and DMA. The halidophilicities in protic solvents such as MeOH, EtOH, and 1-PrOH that solvate halide ions and DMF that solvates or coordinates to Cu^{II} species are relatively low.

D.3. Unsaturated Cu^{II}/L Complexes with Low Values of Halidophilicity. It was not immediately clear for solvents in which halidophilicity was low (e.g., MeOH) whether the $E_{1/2}$ of the copper bromide complex would give a true estimate of K^{app}_{Halido} when the $Cu^{II}L_n$ species were not saturated with Br^-. In other words, would two distinct potentials be observed, or rather a kind of average $E_{1/2}$ be seen, when both $[Cu^{II}/L]^{2+}$ and $[Cu^{II}Br/L]^{+}$ were present in solution? This question is definitively answered by the data presented in Table 6, which is further illustrated in Figure 4. When a substoichiometric amount of Br^- relative to Cu is present, two distinct redox processes are observed that are separated by ~230 mV. It is clearly seen that by increasing the ratio $[Br^-]/[Cu^{II}L_n]$ from 0 to 0.33, 0.5, 0.67, and 2.0, the relative intensity of the $[Cu^{II}/L]^{2+}/[Cu^{I}/L]^{+}$ couple decreases while that of the $[Cu^{II}Br/L]^{+}/[Cu^{I}/L]Br$ couple increases, yet the $E_{1/2}$ values for each process remain essentially constant through all measurements. The data importantly and conclusively demonstrate that even if the "noncoordinating" perchlorate electrolyte present in large excess displaces some of the halide anion, or if the halide anion partially dissociates because it is well solvated in a given solvent, reliable values of the $[Cu^{II}Br/L]^{+}/[Cu^{I}/L]^{+}Br^-$ couple can still be attained.

E. Predicting Solvent Effects. *E.1. Correlation of All Thermodynamic Parameters.* Analysis of the data demonstrates that by measuring values of $E_{1/2}$ of the catalyst and by calculating relative values of K_{EA} from the literature, one can accurately explain and even predict values of K_{ATRP} in a given solvent. For example, the equilibrium constant of electron transfer for $Cu^{II}Br_2$/HMTETA is ~3.3 orders of magnitude greater in MeCN than in MeOH (Table 4). However, this is well balanced by the fact that K_{EA} of the bromine atom is 3.5 orders of magnitude greater in MeOH than in MeCN (Table 2). One would predict, based on this

Table 6. Titration of $Cu^{II}(CF_3SO_3)_2$/TPMA with NBu_4Br in MeCN[a]

	$Cu(CF_3SO_3)$				CuBr			
$[Br^-]/[Cu^{II}L_n]$	$E_{p,a}$ [V]	$E_{p,c}$ [V]	ΔE_p [mV]	$E_{1/2}$ [V]	$E_{p,a}$ [V]	$E_{p,c}$ [V]	ΔE_p [mV]	$E_{1/2}$ [V]
0	−0.290	−0.359	69	−0.325				
0.33	−0.294	−0.360	66	−0.327	−0.523	−0.593	70	−0.558
0.5	−0.293	−0.355	62	−0.324	−0.516	−0.590	74	−0.553
0.67	−0.298	−0.360	62	−0.329	−0.516	−0.595	79	−0.556
2.0					−0.535	−0.607	72	−0.571

[a] 0.1 M NBu_4ClO_4, 1.0 mM $Cu^{II}(CF_3SO_3)_2$/TPMA complex, scan rate 0.10 V s^{-1}; potentials reported vs 0.01 M $AgClO_4$; $E_{p,a}$ and $E_{p,c}$ are the peak potentials of the oxidation and reduction waves, respectively. $E_{1/2} = (E_{p,a} + E_{p,c})/2$.

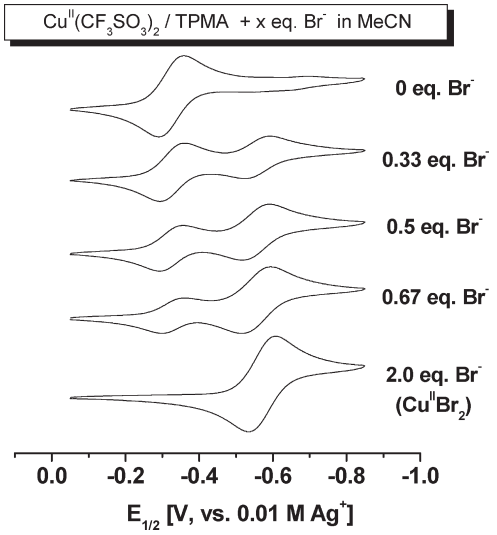

Figure 4. Cyclic voltammograms measured for 1.0 mM $Cu^{II}(CF_3SO_3)_2$/L with increasing amounts of NBu_4Br in MeCN at 25 °C.

information, that K_{ATRP} of Cu^IBr/HMTETA should differ by less than a factor of 2 in MeCN and MeOH, and indeed this is the case (Table 1). In DMSO, the equilibrium constant of electron transfer for $Cu^{II}Br_2$/HMTETA is 4.1 orders of magnitude greater than in MeOH, while K_{EA} in MeOH is 2.8 orders of magnitude greater than in DMSO. One would therefore predict K_{ATRP} should be ~1.3 orders of magnitude greater in DMSO than in MeOH. The experimental data very closely reflect this, with K_{ATRP} being 1.45 orders of magnitude greater in DMSO.

The data in Tables 1 (K_{ATRP}), 2 (K_{EA}), and 4 (K^{app}_{Halido}/K_{ET}) are more fully illustrated in Figure 5, where K_{BH} in the equation $K_{ATRP} = (K_{EA}K_{BH}K^{app}_{Halido})/K_{ET}$ is assumed constant among the different solvents. In Figure 5a, eq 3 has been rearranged to emphasize that even though values of K_{EA} vary by nearly 6 orders of magnitude among the different solvents, K_{ATRP} is well predicted knowing the redox potential of the complex in a given solvent. The plot in Figure 5b was arranged in similar fashion to emphasize the dramatic difference in solvent dependence of K^{app}_{Halido}/K_{ET} obtained from redox potential measurements. The slope of the double-logarithmic dependence in both of these plots is very near unity ($m = 0.99$), demonstrating the self-consistency of Scheme 2 in all of the solvents. Figure 5c is more useful for directly predicting values of K_{ATRP} from the redox potential of the catalyst and K_{EA} available from the literature data.

In Figure 5, the values of K^{app}_{Halido} rather than K_{Halido} are used, since the former are easily obtained from electrochemical measurements, whereas to calculate the latter, knowledge of the value of K_{ATRP} is needed and experimental determination requires time-consuming titrations.[42] This does, however, make the data subject to discrepancies in

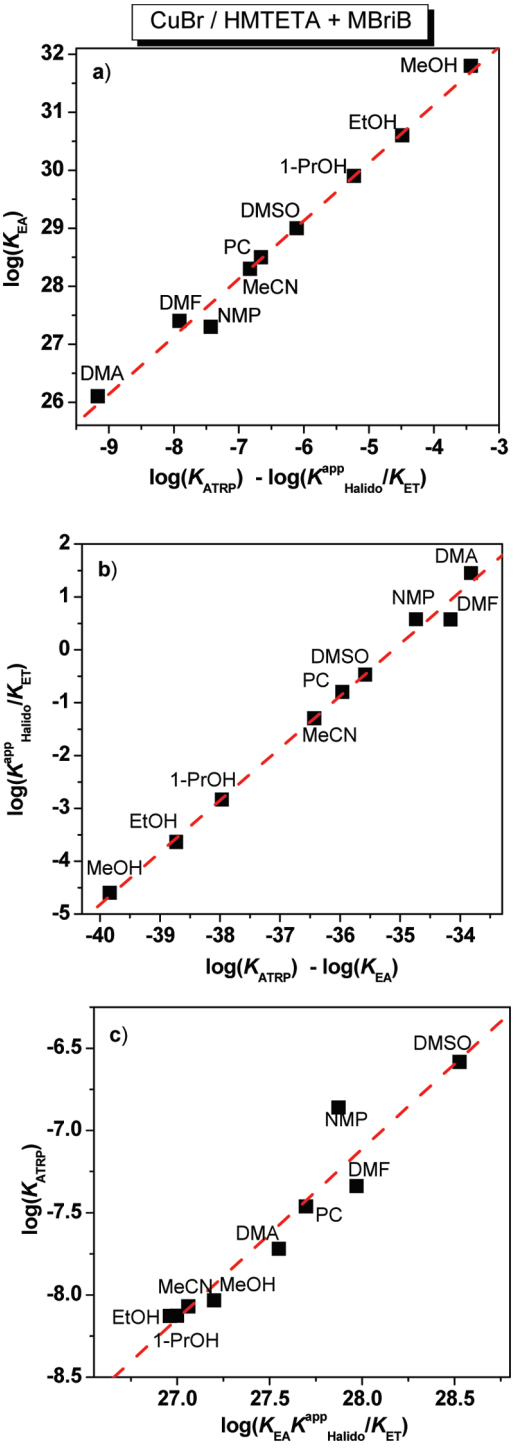

Figure 5. Values of K_{ATRP} measured for Cu^IBr/HMTETA with MBriB; K_{EA} of Br calculated from literature; K_{Halido}/K_{ET} calculated from $E_{1/2}$ measured for $Cu^{II}Br_2$/HMTETA; value for acetone omitted.

Cu^I halidophilicities. For example, in Figure 5c, the measured value of K_{ATRP} in NMP is about 0.5 orders of magnitude higher than predicted, and the measured value in acetone is higher than predicted by 1.5 orders of magnitude. This is wholly consistent with the fact that the Cu^I halidophilicity in NMP and acetone are approximately 0.5 and 1.5 orders of magnitude higher than in the other eight solvents (see Table 5 and its discussion), causing the underestimation of K_{ATRP} in these solvents.

The equilibrium constant for alkyl halide bond homolysis (K_{BH}) is assumed to be solvent independent in the presentation of the data in Figure 5; in reality, these values may vary by as much as a half an order of magnitude and could contribute as a source of error. Regardless, this work clearly demonstrates that ATRP catalyst activity can be explained in a given solvent as a function of reducing power of the complex and the electron affinity of the halide anion in a particular solvent.

E.2. Linear Solvation Energy Relationships. The Kamlet−Taft expression,[49] as shown in eq 9, is a linear solvation energy relationship that has been successfully used to describe and predict properties in solution such as solubility, free energy and enthalpy of equilibria, and redox potentials.

$$XYZ = XYZ_0 + a\alpha + b\beta + s\pi^* + h(\delta_H)^2 \qquad (9)$$

In this equation, XYZ is the property of interest (e.g., the redox potential); XYZ_0, a, b, s, and h are solvent-independent coefficients characteristic of the process; α is the hydrogen bond donor ability of the solvent; β is the hydrogen bond acceptor ability; π^* is a polarizability parameter, which quantifies the ability of the solvent to stabilize a charge or dipole by virtue of its dielectric effect; and $(\delta_H)^2$ is the squared Hildebrand solubility parameter, which is a measure of solvent−solvent interactions that are interrupted in creating a cavity for the solute. Rather than being based on solvent effects on single indicators, these solvatochromic parameters, mentioned above and gathered in Table 7, were arrived at by averaging multiple normalized solvent effects on a variety of properties involving many diverse types of indicators, including rate and equilibrium constants, fluorescence lifetimes, positions and intensities of maximal absorption in NMR, ESR, IR, and UV/vis spectra, NMR coupling constants, free energies and enthalpies of solution and of transfer of dipolar solutes between solvents, enthalpies and free energies of formation of hydrogen-bonded and Lewis acid−base complexes, etc.[50] Other solvatochromic parameters have been proposed and used in the literature, including (but not limited to) a "polarizability correction term", $s(\pi^* + d\delta)$, applied to polychlorinated and aromatic solvents; a measure of coordinate covalency, $e\xi$, applied to P═O, single-bonded oxygen, pyridine, and sp^3-hybridized

Table 7. Solvatochromic Parameters of Solvents[49,52] and Predicted Values of log(K_{ATRP})

solvent	H-bond donor ability (α)	H-bond acceptor ability (β)	polarizability (π^*)	Hildebrand parameter $(\delta_H)^2$	predicted log(K_{ATRP})[a]
alcohols and water					
ethanol	0.83	0.75	0.54	162.1	−8.12 (−8.13)
ethylene glycol	0.9	0.52	0.92	274	−6.71
methanol	0.93	0.66	0.6	205.2	−7.79 (−8.03)
1-propanol	0.78	0.8	0.52	143.2	−8.23 (−8.07)
2-propanol	0.76	0.95	0.48	133.1	−8.12 (−8.16)
water	1.17	0.18	1.09	549	−4.23
amides					
dimethylacetamide	0	0.76	0.88	116.6	−7.35 (−7.72)
dimethylformamide	0	0.69	0.88	138.9	−7.24 (−7.34)
formamide	0.71	0.6	0.97	368.6	−5.29
hexamethylphosphoramide	0	1.05	0.87	73.4	−7.31
N-methylpyrrolidone	0	0.77	0.92	127.6	−7.15 (−6.86)
aromatic hydrocarbons					
benzene	0	0.10	0.59	84.6	−9.41
toluene	0	0.11	0.54	79.4	−9.54
o-xylene	0	0.12	0.47	80.8	−9.62
esters					
ethyl acetate	0	0.45	0.55	79.2	−8.90
propylene carbonate	0	0.4	0.83	176.9	−7.43
ethers					
anisole	0	0.22	0.73	92.9	−8.86
dioxane	0	0.37	0.55	100	−8.82
tetrahydrofuran	0	0.55	0.58	86.4	−8.59
halo compounds					
1-bromobutane	0	0	0.48	75.5	−9.88
hexafluoro-2-propanol	1.96	0	0.65	89.3	−11.01
trifluoroethanol	1.51	0	0.73	137.1	−9.98
ketones					
acetone	0.08	0.48	0.71	98	−8.43 (−8.50)
acetophenone	0	0.49	0.9	103.7	−7.95
butanone	0.06	0.48	0.67	86	−8.61
cyclohexanone	0	0.53	0.76	98	−8.18
nitriles					
acetonitrile	0.19	0.4	0.75	137.8	−8.15 (−8.13)
benzonitrile	0	0.37	0.9	122.9	−7.96
sulfoxides					
dimethyl sulfoxide	0	0.76	1	168.8	−6.57 (−6.58)

[a] Values predicted by the Kamlet−Taft relationship where $XYZ = -11.54 - 0.80\alpha + 1.83\beta + 1.72\pi^* + 0.011(\delta_H)^2$, determined from a regression of the solvatochromic parameters in this table and the K_{ATRP} data from 11 solvents in Table 1. The numbers in parentheses are experimentally determined.

amine bases.[50] Other parameters that are related to the ones mentioned above include Gutmann's donor and acceptor numbers (DN and AN);[51] the reciprocal of the solvent's dielectric constant, $1/\varepsilon$ (Born's function describing ion−ion interactions), or the more complex $(\varepsilon - 1)/(2\varepsilon + 1)$ (Kirkwood's function for ion−dipole interactions);[29] and the molar volume of the solvent.[49]

Ideally, multivariable linear regressions for a given process should involve the minimum number of variables, and all of the aforementioned variables are likely unnecessary to adequately describe the processes in this work. Through Kamlet and Taft's judicious choice of solvents, reactants, and the vast array of other indicators mentioned above to determine the generally agreed upon values of the α, β, and π^* parameters,[50] they demonstrated a more manageable form of a linear solvation energy relationship could be used neglecting the parameters δ and ξ. In general, it was found in this work that by using only the α, β, π^*, and $(\delta_H)^2$ parameters, reasonable values for the multiple correlation coefficient squared, R^2, could be obtained in the multivariable linear regressions for the processes defined by K_{EA} of the three halide anions and K^{app}_{Halido}/K_{ET} of $Cu^{II}Br_2$/HMTETA ($R^2 \geq 0.95$). For K^{app}_{Halido}/K_{ET} of the Cu^{II}/TPMA complex and K_{ATRP} of $Cu^{I}Br$/HMTETA reacting with MBriB, R^2 is between 0.90 and 0.95. The R^2 values of the latter two processes would likely be improved by including more solvent parameters but were not explored any further in this work.

In a recent study,[39] the solvent independent coefficients XYZ_0, a, b, s, and h were determined for the redox potentials of six different $Cu^{I}Br$/L complexes by measuring the $E_{1/2}$ of each complex in six different solvents. To demonstrate the reliability of the coefficients obtained from a multivariable linear regression analysis of the data, the measured redox potentials were then plotted against those predicted using eq 8, which ideally should generate a line with slope = 1.0. The observed good linear correlation ($R^2 \geq 0.96$) along this line suggested that $E_{1/2}$ values could indeed be reliably predicted in other solvents not measured in the study. In analogous manner, a multivariable linear regression was performed in this work to determine XYZ_0, a, b, s, and h for the experimental processes defined by K^{app}_{Halido}/K_{ET} (from $E_{1/2}$ of $Cu^{II}Br_2$/HMTETA and $Cu^{II}Br_2$/TPMA) and also K_{ATRP} of $Cu^{I}Br$/HMTETA reacting with MBriB. Predicted values of K^{app}_{Halido}/K_{ET} and K_{ATRP} using the derived Kamlet−Taft relationship were then correlated with those values actually measured in Figures 6 and 7, respectively. A summary of the solvent independent coefficients determined from the regression is provided in Table 8. To further illustrate the usefulness of this predictive tool, K_{ATRP} was predicted in 17 more organic solvents and water using the appropriate solvatochromic parameters from Table 7. A sample of the predicted K_{ATRP} values of these solvents is also illustrated in Figure 7, but for the sake of clarity, many are only presented in the table.

In order to readily compare the relative contributions of each of the solvent properties in the overall process, so-called beta coefficients are employed in the Supporting Information to extract physiochemical information from the Kamlet−Taft relationships. The results are summarized in Table S2, followed by significant discussion of the relative importance of all the parameters in each process.

As can be seen in Figure 7, the use of the multivariable linear regression has allowed the extrapolation of ATRP catalyst activity nearly 7 orders of magnitude, from 10^{-11} in fluoroalcohols to nearly 10^{-4} in water. In general, K_{ATRP} ranges between 10^{-9} and 10^{-10} in aromatic hydrocarbons, between 10^{-8} and 10^{-9} in ethers, ketones, and nitriles, is $\sim 10^{-8}$ in most alcohols, and is between 10^{-7} and 10^{-8} for most amides. A few exceptions where K_{ATRP} is quite high include formamide and ethylene glycol, an observation

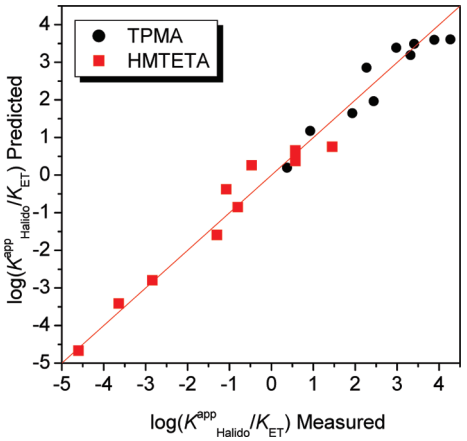

Figure 6. $\text{Log}(K^{app}_{Halido}/K_{ET})$ values measured in this article (from values of $E_{1/2}$ and transfer energies available in the literature[36]) are plotted against values predicted by the Kamlet−Taft relationship where $XYZ = 5.48 - 6.91\alpha + 4.62\beta - 7.97\pi^* + 0.014(\delta_H)^2$ for $Cu^{II}Br_2$/TPMA and $XYZ = 0.18 - 5.72\alpha + 4.11\beta - 2.37\pi^* - 0.004(\delta_H)^2$ for $Cu^{II}Br_2$/HMTETA. The line represents values predicted by the Kamlet−Taft relationship.

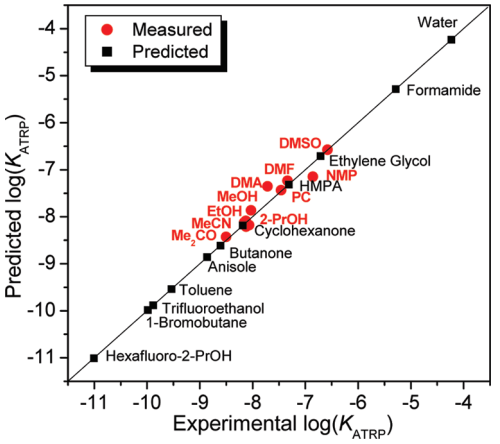

Figure 7. $\text{Log}(K_{ATRP})$ values measured in this article for $Cu^{I}Br$/HMTETA + MBriB are plotted against values predicted by the Kamlet−Taft relationship where $XYZ = -11.54 - 0.80\alpha + 1.83\beta + 1.72\pi^* + 0.011(\delta_H)^2$. The line represents values predicted by the Kamlet−Taft relationship. Predicted values of K_{ATRP} for 15 organic solvents and water are also provided based on these solvent-independent coefficients and the appropriate solvatochromic parameters from Table 7.

Table 8. Solvent-Independent Coefficients Determined for Logarithmic Values of K^{app}_{Halido}/K_{ET} for $Cu^{II}Br_2$/TPMA and $Cu^{II}Br_2$/HMTETA and K_{ATRP} for $Cu^{I}Br$/HMTETA with MBriB

equilibrium constant	XYZ_0	$a(\alpha)$	$b(\beta)$	$s(\pi^*)$	$h(\delta_H)^2$	R^2
$\log(K^{app}_{Halido}/K_{ET})$ for $Cu^{II}Br_2$/TPMA	5.48 ± 2.60	-6.91 ± 2.91	4.62 ± 2.20	-7.97 ± 5.79	0.014 ± 0.013	0.901
$\log(K^{app}_{Halido}/K_{ET})$ for $Cu^{II}Br_2$/HMTETA	0.18 ± 2.85	-5.72 ± 3.18	4.11 ± 2.40	-2.37 ± 6.34	-0.004 ± 0.015	0.951
$\log(K_{ATRP})$ for $Cu^{I}Br$/HMTETA with MBriB	-11.54 ± 0.83	-0.80 ± 0.86	1.83 ± 0.55	1.72 ± 1.61	0.011 ± 0.005	0.925

which could have important implications for those seeking conditions to mediate ATRP of less reactive monomers.

Conclusions

The ATRP equilibrium constant is an excellent measure of catalyst activity with a given alkyl halide in this polymerization technique. As the value of K_{ATRP} ultimately governs the rate of polymerization, with knowledge of this constant, one can appropriately match the activity of a catalyst with the reactivity of a monomer and can even calculate whether polymerization will occur on a feasible time scale when less reactive monomers are used. A model representing thermodynamic activity in ATRP as the product of alkyl halide bond homolysis and three other distinct thermodynamic contributions related to the catalyst was rigorously evaluated, including the reduction/oxidation of both the metal complex and the halogen atom as well as the affinity of the catalyst for halide anions (or "halidophilicity"). The validity and self-consistency of the equation $K_{ATRP} = (K_{BH}K_{EA}K_{Halido})/K_{ET}$ was verified by independently measuring, computing, or calculating all five equilibrium constants for one catalyst/alkyl halide in MeCN.

It is envisioned that this model will prove particularly important to future developments of the ATRP catalyst. Previous research demonstrated the correlation between polymerization activity in ATRP and the redox potential of the catalyst. This model takes the next step by allowing precise calculation of catalyst activity, often with values of reduction/oxidation of both the metal complex and the halogen atom that are already available in the literature. As a thorough demonstration of the value and effectiveness of this model, the equilibrium constants K_{ATRP}, K_{EA}, and K^{app}_{Halido}/K_{ET} were measured/calculated in 10 different organic solvents, and their values were used to both understand and predict catalyst activity in ATRP. Furthermore, the solvent effects were quantitatively analyzed in terms of Kamlet−Taft parameters, and linear solvation energy relationships were employed to extrapolate catalyst activity over 7 orders of magnitude in 17 more organic solvents and water.

Acknowledgment. The authors thank the members of the ATRP/CRP consortia at Carnegie Mellon University and NSF (Grants CHE-0715494 and DMR-0549353) for funding. W.A.B. thanks the Harrison Legacy Dissertation Fellowship for financial support. Drs. Gayathri C. Withers and Roberto R. Gil are acknowledged for help with the DOSY NMR experiments.

Supporting Information Available: Table of cyclic voltammetry data for $Cu^{II}(CF_3SO_3)_2$/L complexes in MeCN; DOSY NMR spectra used in diffusion coefficient measurements; electronic spectra of all relevant compounds; plots used in the determination of all K_{ATRP} values. This material is available free of charge via the Internet at http://pubs.acs.org.

References and Notes

(1) Braunecker, W. A.; Matyjaszewski, K. *Prog. Polym. Sci.* **2007**, *32*, 93–146.
(2) Wang, J.-S.; Matyjaszewski, K. *J. Am. Chem. Soc.* **1995**, *117*, 5614–5615.
(3) Tsarevsky, N. V.; Tang, W.; Brooks, S. J.; Matyjaszewski, K. *ACS Symp. Ser.* **2006**, *944*, 56–70.
(4) Tsarevsky, N. V.; Matyjaszewski, K. *Chem. Rev.* **2007**, *107*, 2270–2299.
(5) Matyjaszewski, K.; Xia, J. *Chem. Rev.* **2001**, *101*, 2921–2990.
(6) Kamigaito, M.; Ando, T.; Sawamoto, M. *Chem. Rev.* **2001**, *101*, 3689–3745.
(7) Perrier, S.; Haddleton, D. M. *Macromol. Symp.* **2002**, *182*, 261–272.
(8) Percec, V.; Guliashvili, T.; Ladislaw, J. S.; Wistrand, A.; Stjerndahl, A.; Sienkowska, M. J.; Monteiro, M. J.; Sahoo, S. *J. Am. Chem. Soc.* **2006**, *128*, 14156–14165.
(9) Pintauer, T.; McKenzie, B.; Matyjaszewski, K. *ACS Symp. Ser.* **2003**, *854*, 130–147.
(10) Braunecker, W. A.; Tsarevsky, N. V.; Gennaro, A.; Matyjaszewski, K. *Polym. Prepr. (Am. Chem. Soc., Div. Polym. Chem.)* **2008**, *49*, 376–377.
(11) (a) Tang, W.; Matyjaszewski, K. *Macromolecules* **2006**, *39*, 4953–4959. (b) Tang, W.; Tsarevsky, N. V.; Matyjaszewski, K. *J. Am. Chem. Soc.* **2006**, *128*, 1598–1604. (c) Ohno, K.; Goto, A.; Fukuda, T.; Xia, J.; Matyjaszewski, K. *Macromolecules* **1998**, *31*, 2699–2701. (d) Arehart, S. V.; Matyjaszewski, K. *Macromolecules* **1999**, *32*, 2221–2231. (e) Matyjaszewski, K.; Paik, H.-j.; Zhou, P.; Diamanti, S. J. *Macromolecules* **2001**, *34*, 5125–5131. (f) Ziegler, M. J.; Matyjaszewski, K. *Macromolecules* **2001**, *34*, 415–424. (g) Pintauer, T.; Matyjaszewski, K. *Coord. Chem. Rev.* **2005**, *249*, 1155–1184.
(12) Tang, W.; Kwak, Y.; Braunecker, W.; Tsarevsky, N. V.; Coote, M. L.; Matyjaszewski, K. *J. Am. Chem. Soc.* **2008**, *130*, 10702–10713.
(13) Tang, W.; Tsarevsky, N. V.; Matyjaszewski, K. *J. Am. Chem. Soc.* **2006**, *128*, 1598–1604.
(14) Braunecker, W. A.; Brown, W. C.; Morelli, B. C.; Tang, W.; Poli, R.; Matyjaszewski, K. *Macromolecules* **2007**, *40*, 8576–8585.
(15) Gillies, M. B.; Matyjaszewski, K.; Norrby, P.-O.; Pintauer, T.; Poli, R.; Richard, P. *Macromolecules* **2003**, *36*, 8551–8559.
(16) Lin, C. Y.; Coote, M. L.; Gennaro, A.; Matyjaszewski, K. *J. Am. Chem. Soc.* **2008**, *130*, 12762–12774.
(17) Qiu, J.; Matyjaszewski, K.; Thouin, L.; Amatore, C. *Macromol. Chem. Phys.* **2000**, *201*, 1625–1631.
(18) Matyjaszewski, K.; Goebelt, B.; Paik, H.-j.; Horwitz, C. P. *Macromolecules* **2001**, *34*, 430–440.
(19) Tang, H.; Arulsamy, N.; Sun, J.; Radosz, M.; Shen, Y.; Tsarevsky, N. V.; Braunecker, W. A.; Tang, W.; Matyjaszewski, K. *J. Am. Chem. Soc.* **2006**, *128*, 16277–16285.
(20) Tsarevsky, N. V.; Braunecker, W. A.; Tang, W.; Brooks, S. J.; Matyjaszewski, K.; Weisman, G. R.; Wong, E. H. *J. Mol. Catal. A: Chem.* **2006**, *257*, 132–140.
(21) Coullerez, G.; Carlmark, A.; Malmstroem, E.; Jonsson, M. *J. Phys. Chem. A* **2004**, *108*, 7129–7131.
(22) O'Reilly, R. K.; Gibson, V. C.; White, A. J. P.; Williams, D. J. *J. Am. Chem. Soc.* **2003**, *125*, 8450–8451.
(23) O'Reilly, R. K.; Gibson, V. C.; White, A. J. P.; Williams, D. J. *Polyhedron* **2004**, *23*, 2921–2928.
(24) Ando, T.; Kamigaito, M.; Sawamoto, M. *Macromolecules* **2000**, *33*, 5825–5829.
(25) Richel, A.; Demonceau, A.; Noels, A. F. *Tetrahedron Lett.* **2006**, *47*, 2077–2081.
(26) Bergenudd, H.; Coullerez, G.; Jonsson, M.; Malmstroem, E. *Macromolecules* **2009**, *42*, 3302–3308.
(27) Anderegg, G.; Wenk, F. *Helv. Chim. Acta* **1967**, *50*, 2330.
(28) Holz, M.; Mao, X.-a.; Seiferling, D.; Sacco, A. *J. Chem. Phys.* **1996**, *104*, 669.
(29) Izutsu, K. *Electrochemistry in Nonaqueous Solvents*; Wiley-VCH: Weinheim, 2002.
(30) Tsarevsky, N. V.; Braunecker, W. A.; Matyjaszewski, K. *J. Organomet. Chem.* **2007**, *692*, 3212–3222.
(31) Matyjaszewski, K.; Tsarevsky, N. V.; Braunecker, W. A.; Dong, H.; Huang, J.; Jakubowski, W.; Kwak, Y.; Nicolay, R.; Tang, W.; Yoon, J. A. *Macromolecules* **2007**, *40*, 7795–7806.
(32) Tsarevsky, N. V.; Braunecker, W. A.; Brooks, S. J.; Matyjaszewski, K. *Macromolecules* **2006**, *39*, 6817–6824.
(33) Matyjaszewski, K.; Jakubowski, W.; Min, K.; Tang, W.; Huang, J.; Braunecker, W. A.; Tsarevsky, N. V. *Proc. Natl. Acad. Sci. U.S.A.* **2006**, *103*, 15309–15314.
(34) (a) Jakubowski, W.; Matyjaszewski, K. *Angew. Chem.* **2006**, *45*, 4482–4486. (b) Jakubowski, W.; Min, K.; Matyjaszewski, K. *Macromolecules* **2006**, *39*, 39–45. (c) Jakubowski, W.; Matyjaszewski, K. *Macromolecules* **2005**, *38*, 4139–4146. (d) Min, K.; Gao, H.; Matyjaszewski, K. *J. Am. Chem. Soc.* **2005**, *127*, 3825–3830. (e) Matyjaszewski, K.; Dong, H.; Jakubowski, W.; Pintauer, J.; Kusumo, A. *Langmuir* **2007**, *23*, 4528–4531. (f) Pintauer, T.; Matyjaszewski, K. *Chem. Soc. Rev.* **2008**, *37*, 1087–1097.
(35) Kalidas, C.; Hefter, G.; Marcus, Y. *Chem. Rev.* **2000**, *100*, 819–852.
(36) Marcus, Y. *Pure Appl. Chem.* **1983**, *55*, 977–1021.
(37) Svaan, M.; Parker, V. D. *Acta Chem. Scand. B* **1981**, *B35*, 559–565.

(38) Svaan, M.; Parker, V. D. *Acta Chem. Scand. B* **1982**, *B36*, 351–355.
(39) Coullerez, G.; Malmstrom, E.; Jonsson, M. *J. Phys. Chem. A* **2006**, *110*, 10355–10360.
(40) *Handbook of Chemistry and Physics*, 72nd ed.; CRC: Cleveland, OH, 1991−1992.
(41) Ishiguro, S.; Nagy, L.; Ohtaki, H. *Bull. Chem. Soc. Jpn.* **1987**, *60*, 2053–2058.
(42) Tsarevsky, N. V.; Pintauer, T.; Matyjaszewski, K. *Macromolecules* **2004**, *37*, 9768–9778.
(43) McBryde, W. A. E. *Talanta* **1974**, *21*, 979–1004.
(44) Tsarevsky, N. V.; Braunecker, W. A.; Vacca, A.; Gans, P.; Matyjaszewski, K. *Macromol. Symp.* **2007**, *248*, 60–70.
(45) See Supporting Information.
(46) Lingane, J. J. *Chem. Rev.* **1941**, *29*, 1–35.
(47) Pintauer, T.; Reinoehl, U.; Feth, M.; Bertagnolli, H.; Matyjaszewski, K. *Eur. J. Inorg. Chem.* **2003**, 2082–2094.
(48) Eckenhoff, W. T.; Pintauer, T. *Inorg. Chem.* **2007**, *46*, 5844–5846.
(49) Marcus, Y.; Kamlet, M. J.; Taft, R. W. *J. Phys. Chem.* **1988**, *92*, 3613–3622.
(50) Kamlet, M. J.; Abboud, J. L. M.; Abraham, M. H.; Taft, R. W. *J. Org. Chem.* **1983**, *48*, 2877–2887.
(51) Gutmann, V. *The Donor-Acceptor Approach to Molecular Interactions*; Plenum: New York, 1978.
(52) Barton, A. F. M. *Chem. Rev.* **1975**, *75*, 731–753.